MODELLING OF ICEBERG DRIFT USING WIND AND CURRENT MEASUREMENTS AT A FIXED STATION

ERIC DAVID SOULIS

MODELLING OF ICEBERG DRIFT USING WIND AND CURRENT MEASUREMENTS AT A FIXED STATION.

by

E.D. Soulis, B.A.Sc.

A Thesis submitted in partial fulfillment
of the requirements for the degree of
Master of Engineering

Faculty of Engineering and Applied Science
Memorial University of Newfoundland

November 1976

St. John's Newfoundland,

ABSTRACT

During the summer of 1972 a major oceanographic investigation was conducted in the Labrador Sea by the Faculty of Engineering and Applied Science of Memorial University of Newfoundland. Wind velocity measurements taken at sea and on shore, current velocity measurements from a fixed array of current meters, and iceberg trajectory measurements recorded from a shore based radar are analysed. A statistical study shows that an iceberg's movement can be modelled within 20% from wind and current measurements. The average response of icebergs to wind and transitory current effects is presented.

ACKNOWLEDGEMENTS

I wish to thank the many members of the Faculty of Engineering of Memorial University of Newfoundland who contributed to this study, often unknowingly, with their encouragement and advice, especially my supervisor, Dr. R.T. Dempster, who collected and made available the iceberg tracking data, Dr. J. Allen who directed collection of the oceanographic data, and Prof. N. Durdle, who provided the digital filter applied to the current meter data.

I also wish to acknowledge fellow graduate student Brendan Holden, who prepared the current meter data and with whom many fruitful hours were spent sharing ideas.

Finally, the National Research Council is to be thanked for the financial support I received during my graduate studies.

TABLE OF CONTENTS

TABLE OF CONTENTS (Cont'd)

LIST OF TABLES

LIST OF FIGURES

1. INTRODUCTION

Identification of the hydrocarbon potential of the Labrador continental shelf faced the offshore drilling industry with the unique environmental hazard of icebergs. Since the sinking of the Titanic in 1912 considerable information about general iceberg behaviour has been collected by, for example, the Marion Expedition (Smith, 1931) and, subsequently, the International Ice Patrol (Murray, 1969). The objectives of these studies were, however, to protect shipping and the results are generally synoptic and not designed to provide the details of iceberg behaviour necessary for safe drilling and production operations in iceberg invested waters. The considerable work undertaken to fill this gap was summarized by Bruneau (1973).

The feasible methods for safe drilling operations were explored by Bruneau and Dempster (1972). From the alternatives, the industry has opted to tow smaller bergs when weather permits and to use dynamically positioned drillships, which can leave and re-enter a drill-hole when threatened by a berg (Ainslie, 1974). The lead time required to vacate a hole is of the order of 2 hours and depends on the stage of the drilling program. Both strategies require a means to identify a dangerous iceberg with sufficient lead time to adopt a defensive action.

This suggests a model is needed which relates easily measured environmental parameters to expected iceberg drift.

Motion of an iceberg is, unfortunately, extremely complicated. An iceberg can be considered a solid object, whose shape and orientation are not constant, moving at the interface of two fluids each with highly complex and interrelated velocity fields. Also, an iceberg has mass. Therefore, its future drift depends on its past motion, which in turn depends on the history of wind and current forces it has experienced, as well as the present and future values for the same forces. The response of an iceberg to environmental factors follows the laws of fluid dynamics and changes with the changing shape and orientation of the iceberg. Considering the complexity of the dynamics of the situation, it is not surprising that studies of detailed iceberg drift (Smith, 1931), (Murray, 1969), (Bruneau and Dempster, 1972), have led only to cautious statements about general iceberg behaviour. The detailed drift of an iceberg is, therefore, unique to that iceberg and the environmental conditions in which it exists (Bruneau, 1973).

The study of detailed iceberg drift is being approached by various investigators from three points of view: theoretical fluid dynamics, (Smith, 1974), statistical correlation with past drift (Ainslie, 1974), (Dempster, 1974), and statistical correlation with environmental factors (Soulis, 1974). The final solution of the drift modelling problem probably lies in the combination of the three approaches since correlation techniques for the observed behaviour of a particular iceberg are essential because of a drift pattern's individuality yet theoretical values are necessary to contribute to initial estimates of iceberg response characteristics and to provide a check on statistically estimated parameters.

This thesis is a study of the cross-correlation between iceberg drift and the driving environmental factors, wind and current. A cross-correlation model is developed and applied to 33 icebergs observed off the coast of Labrador during August 1972.

Simple interpretations of the observed iceberg response characteristics are derived and the average behaviour of the group is compared with observed and theoretical general iceberg behaviour. The time dependence of the correlations is examined, to provide a basis for a forecasting model.

2. OBJECTIVES

The objectives of this study are:

a) to identify, using a simple cross-correlation model, the transfer functions which relate wind and current to iceberg drift.

b) to find the lag time which is most useful for modelling of iceberg drift and, therefore, provide a basis for building a forecasting model using cross-correlation techniques.

c) to interpret the transfer functions in such a way that they can be compared with existing experience.

3. GENERAL FORM OF A VECTOR CROSS-CORRELATION MODEL

Iceberg velocity can be expressed as a simple vector function of current and wind velocity by the following equation:

$$\hat{\underline{b}}(t) = \underline{r} + P\underline{c}(t-t_c) + Q\underline{w}(t-t_w) \qquad (1)$$

$\hat{\underline{b}}(t)$ = estimated iceberg velocity at time t

$\underline{r}$ = a constant vector

P = current vector transformation matrix

$\underline{c}(t-t_c)$ = current velocity at time $t-t_c$

t_c = current lag time

Q = wind vector transformation matrix

$\underline{w}(t-t_w)$ = wind velocity at time $t-t_w$

t_w = wind lag time

Equation (1) is illustrated in Figure 1. Observed iceberg velocity is represented by the vector $\underline{b}$.

If the vectors are resolved into Cartesian components, equation (1) becomes:

$$\begin{bmatrix} \hat{b}_x(t) \\ \hat{b}_y(t) \end{bmatrix} = \begin{bmatrix} r_x \\ r_y \end{bmatrix} + \begin{bmatrix} p_{11} & p_{12} \\ p_{21} & p_{22} \end{bmatrix} \begin{bmatrix} c_x(t-t_c) \\ c_y(t-t_c) \end{bmatrix} + \begin{bmatrix} q_{11} & q_{12} \\ q_{21} & q_{22} \end{bmatrix} \begin{bmatrix} w_x(t-t_w) \\ w_y(t-t_w) \end{bmatrix} \qquad (2)$$

There is no ambiguity created by removing the references to t, t_c, and t_w in equation (2), which can therefore be written:

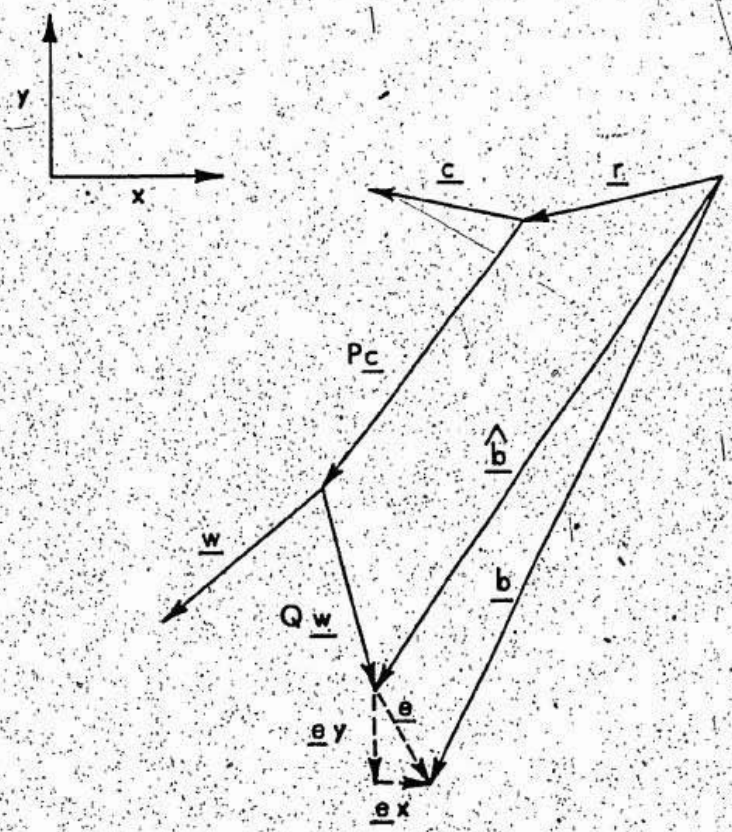

ELEMENTS OF A VECTOR CORRELATION MODEL

Figure 1

$$b_x = r_x + p_{11} c_x + p_{12} c_y + q_{11} w_x + q_{12} w_y \quad (3a)$$

$$b_y = r_y + p_{21} c_x + p_{22} c_y + q_{22} w_x + q_{21} w_y \quad (3b)$$

The objective of this study consequently becomes, for each iceberg for which data is available, to estimate and interpret the values of the parameters in equation (2) which give the best estimates of b_x and b_y, the components of observed iceberg velocity $\underline{b}$.

It is necessary therefore to define a "best estimate". In scalar problems this is usually the estimate that gives the least sum of the squares of residuals between observed and estimated data. In vector problems, the estimate can be derived that gives the least sum of the squares of the magnitudes of the vector residuals. A typical vector residual is illustrated by $\underline{e}$ in Figure 1. Therefore, the best estimates of the elements $\underline{r}$, P and Q and the values of t_c and t_w can be those which minimize:

$$O^2 = \sum_{i=1}^{N} |\underline{e}_i|^2 \quad (4)$$

O^2 = objective function

$\underline{e}_i$ = the ith vector residual

N = number of observations

In this study, the combination of model parameters in equation (2) which minimized O^2 was found for each iceberg by testing, within a reasonable range, all combinations of t_c and t_w. For each combination

the lowest possible O^2 was computed by finding the best choice of elements for $\underline{r}$, P, and Q. The values of t_c and t_w that had the overall lowest O^2 and the corresponding elements of $\underline{r}$, P, and Q were selected as the best estimates of the model parameters.

Computation of the best choice of $\underline{r}$, P, and Q for a given t_c and t_w is a straight forward exercise involving least square techniques. Equation (4) can be written:

$$O^2 = \sum_{i=1}^{N} |\underline{e}_i|^2$$

$$= \sum_{i=1}^{N} (e_{xi}^2 + e_{yi}^2)$$

$$O^2 = \sum_{i=1}^{N} e_{xi}^2 + \sum_{i=1}^{N} e_{yi}^2 \qquad (5)$$

If $\sum_{i=1}^{N} e_{xi}^2$ and $\sum_{i=1}^{N} e_{yi}^2$ are evaluated independently:

$$O^2_{min} = \left(\sum_{i=1}^{N} e_{xi}^2\right)_{min} + \left(\sum_{i=1}^{N} e_{yi}^2\right)_{min} \qquad (6)$$

This condition is met if $\sum_{i=1}^{N} e_{xi}^2$ and $\sum_{i=1}^{N} e_{yi}^2$ are evaluated using equations (3a) and (3b) respectively, since minimization of $\sum_{i=1}^{N} e_{xi}^2$ using equation (3a) neither restricts nor is restricted by the minimization of $\sum_{i=1}^{N} e_{yi}^2$ using equation (3b). Therefore, O^2_{min} for a given t_c and t_w can be calculated by evaluating the elements of $\underline{r}$, P, and Q that give, separately, the best least squares fit to observed data for equations (3a) and (3b).

4. DATA COLLECTION

The data used in this study were collected during a major oceanographic investigation conducted in the summary of 1972 off Saglek, Labrador (see Figure 2) by the Faculty of Engineering and Applied Science of Memorial University of Newfoundland.

Full details of the expedition are given by Allen (1972). Dempster et al (1973) summarize the study as follows:

> "Icebergs were tracked, using radar installed in a shore station at Saglek, Labrador, while the CSS "Dawson" provided by the Bedford Institute, together with the Canadian Armed Services, Maritime Command, collected oceanographical and meteorological data in the vicinity. A total of one hundred and ten icebergs were tracked, some for several days and others for only several hours. In addition, the scientific party aboard the "Dawson" obtained extensive data on directly measured currents in the area, salinity, temperature and depth profiles and also underwater shapes of icebergs. This latter data was collected by acoustically profiling icebergs in the vertical direction from stations located around each iceberg. Maritime Command flew an Argus aircraft over the area to make a large scale infra-red study of the ocean surface, and also to take stereo photographs of the above water portion of selected icebergs."

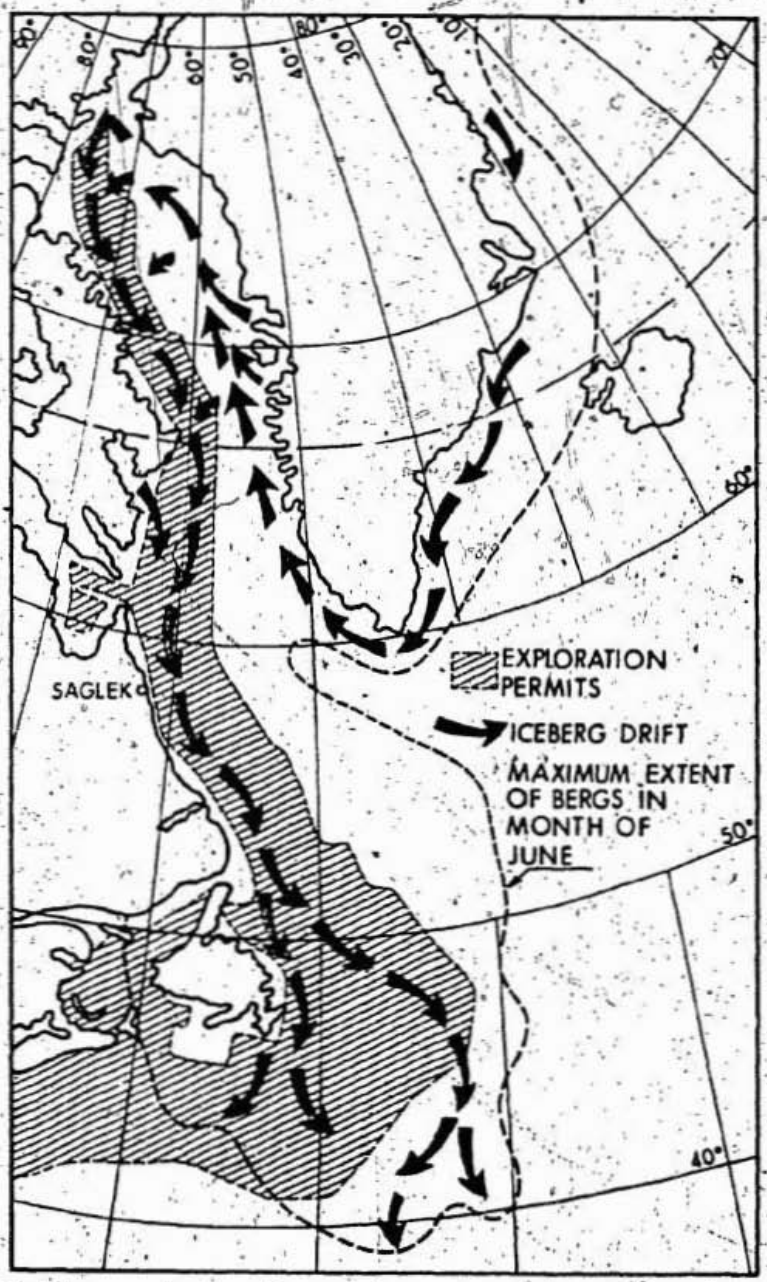

EXTENT AND DRIFT OF ICEBERGS IN THE NORTH ATLANTIC WITH AN INDICATION OF THE EXTENT OF EXPLORATION PERMITS GRANTED BY THE GOVERNMENT OF CANADA.
(from Bruneau and Dempster 1972)

Figure 2

5. DATA PREPARATION

5.1 General

Before comparison of the current, wind, and iceberg velocity vector-time series observed during the Saglek study, some preliminary processing was necessary. This section outlines the procedures used, summarized in Figure 3.

5.2 Current Data

Direct measurement of the current near Saglek is described by Allen (1973). The locations of the current meter strings are shown in Figure 4. Each string was identified by a letter A, B, C or D and consisted of 3 meters, number one 13 m from the ocean-surface, number two at about mid-water, and number three near the ocean bottom. For example, meters A1, B1 and C1 were located 13 meters below the ocean surface at points A, B and C (Figure 4) respectively.

The meters were operated from July 28 to August 25, 1972. Decoding and editing was organized by Holden (1974), who also conducted detailed analysis of the records. The record for meter C1 is shown in Figures 5 and 6. A progressive vector diagram for the same meter is in Figure 7. Unfortunately the mid-water meters all malfunctioned and the results from string D were unavailable during the following analysis. Only meters A1, B1, and C1 were used in this study.

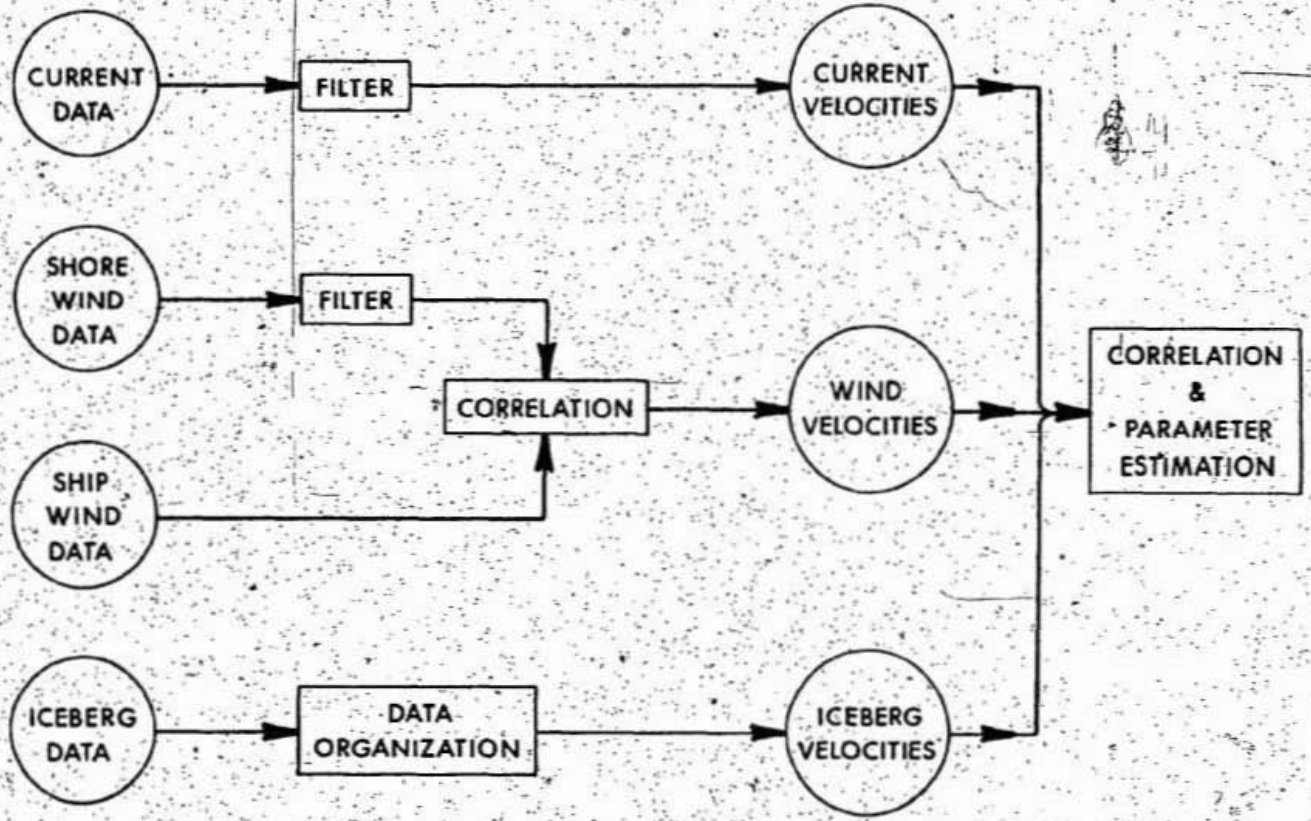

INFORMATION FLOW
SAGLEK ICEBERG STUDY

Figure 3.

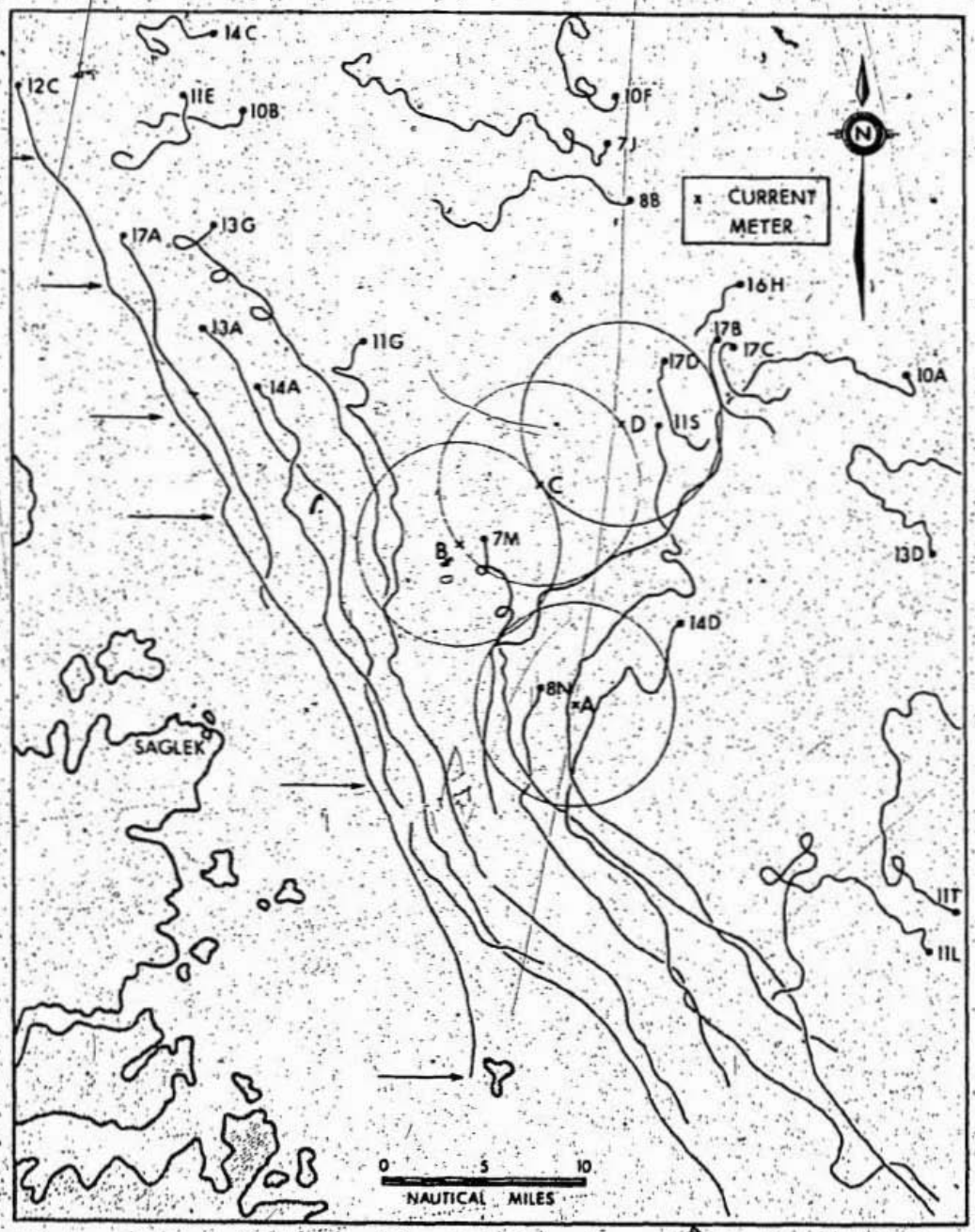

DRIFT PATTERN OF ICEBERGS OFFSHORE SAGLEK SHOWING LOCATION OF CURRENT METERS

Figure 4.

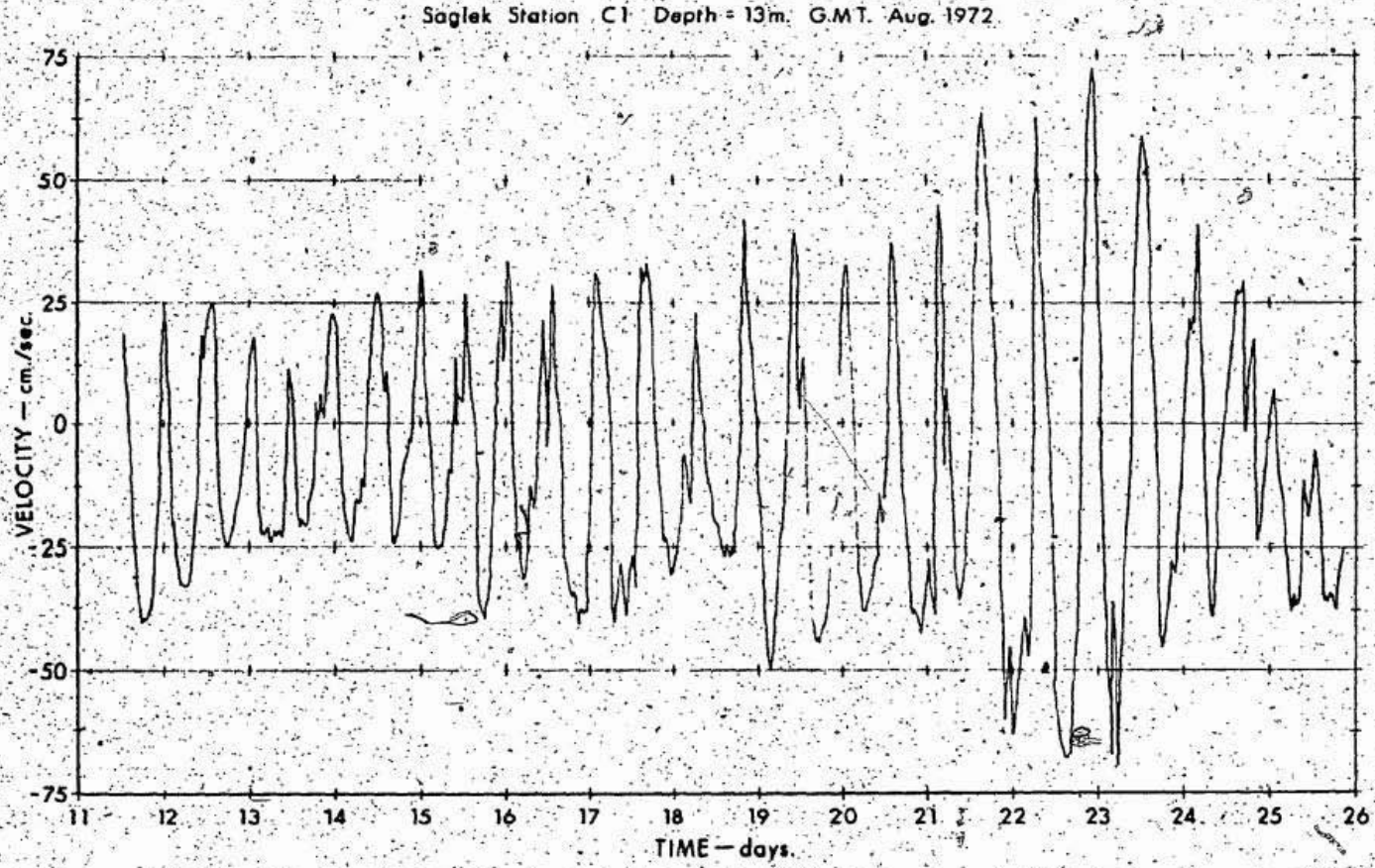

NORTH VELOCITY COMPONENT — METER C1.

Figure 5.

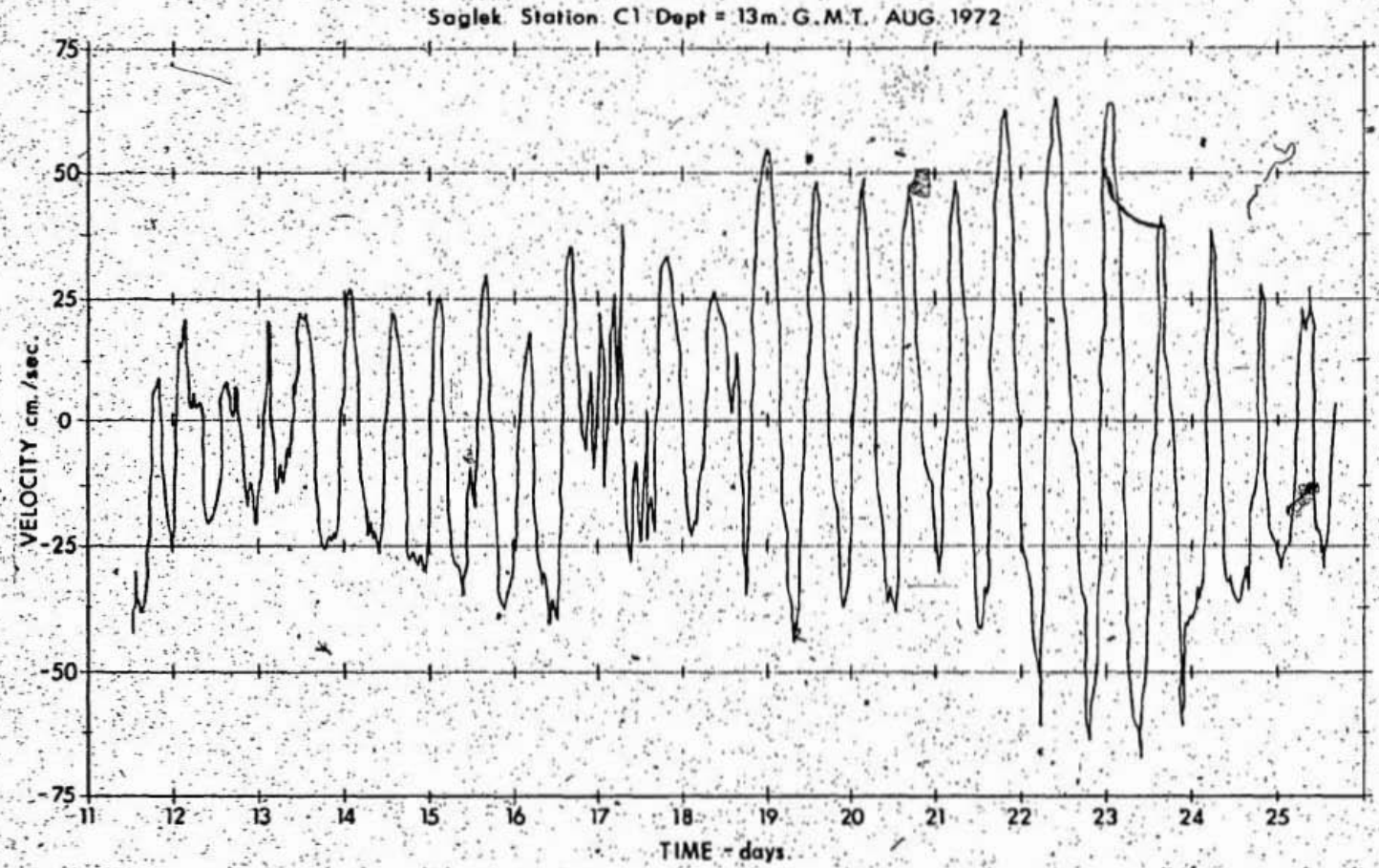

EAST VELOCITY COMPONENT - METER C1

Figure 6

Saglek Station C1 Depth = 13m. G.M.T. Aug. 11-25, 1972

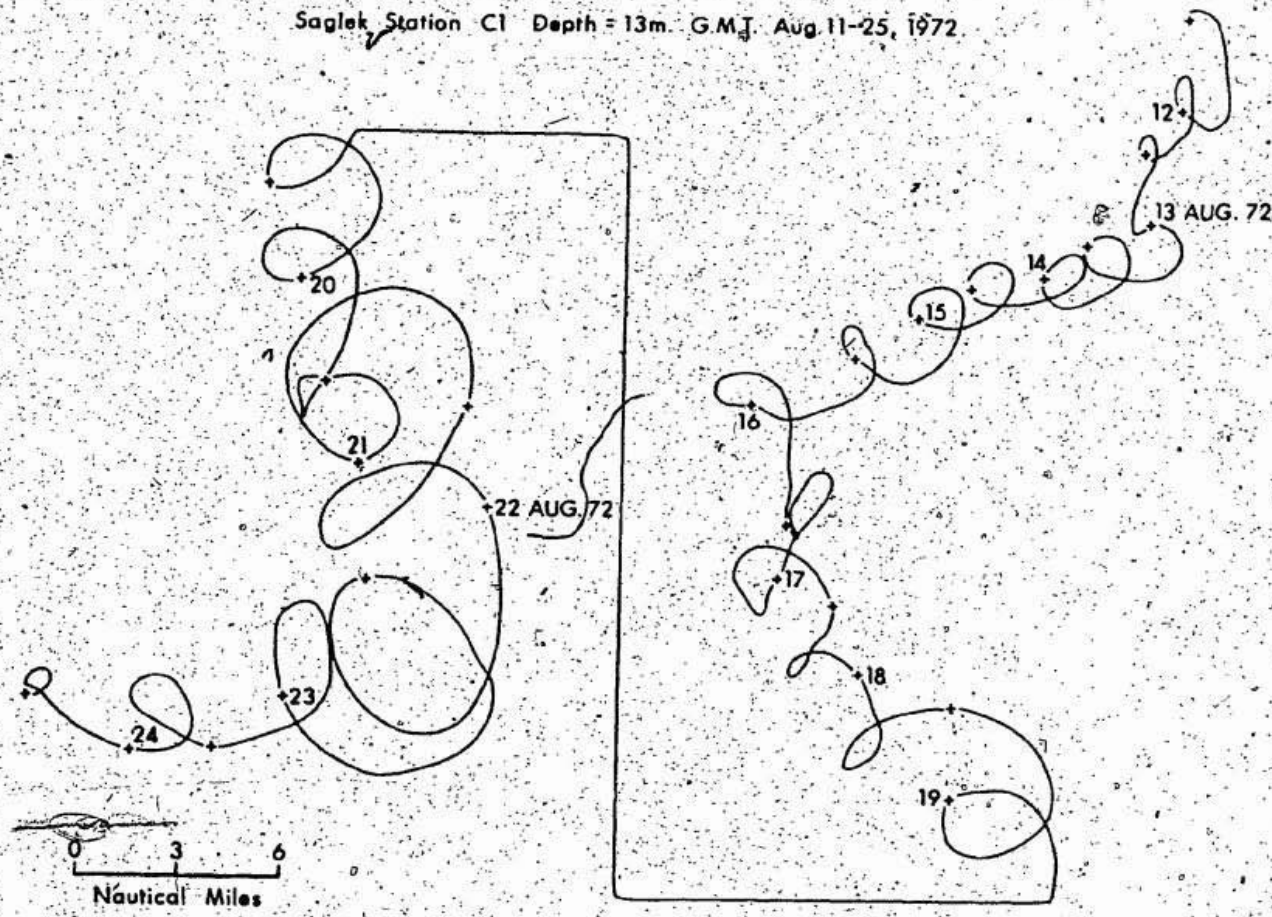

PROGRESSIVE VECTOR DIAGRAM - METER C1

Figure 7

Figure 8 is a power spectrum for the north velocity component of meter C1. All meters showed a similar peak between 12 and 14 hours, which is presumed to represent some combination of the principle semi-diurnal tidal period of 12.43 hours and the inertial period of 14.8 hours (Neumann and Pierson, 1966). The amplitude of the unsteady component varied from 25 to 50 cm/sec, whereas the mean components were all between 2 and 3 cm/sec.

Analysis of the spatial cross-correlation between current records was conducted as part of the preliminary processing of current meter data. The results were useful for the weighting of iceberg observations (sec 5.6.4).

The cross-correlation between records was characterized by the cross-covariance function:

$$\gamma(\tau) = \frac{1}{T} \sum_{t=1}^{T} \frac{(x(t) - \bar{x})(y(t+\tau) - \bar{y})}{s_x s_y}$$

in which x and y are time series with means $\bar{x}$ and $\bar{y}$ and standard deviations s_x and s_y respectively.

For each pair of current meters studied, two such functions exist, one for the north-south velocity components and the other for the east-west components. The functions were sinusoidal with respect to τ with their amplitude decaying slowly as τ increased. The maximum values for $\gamma(\tau)$ usually occurred for τ close to zero. The square root

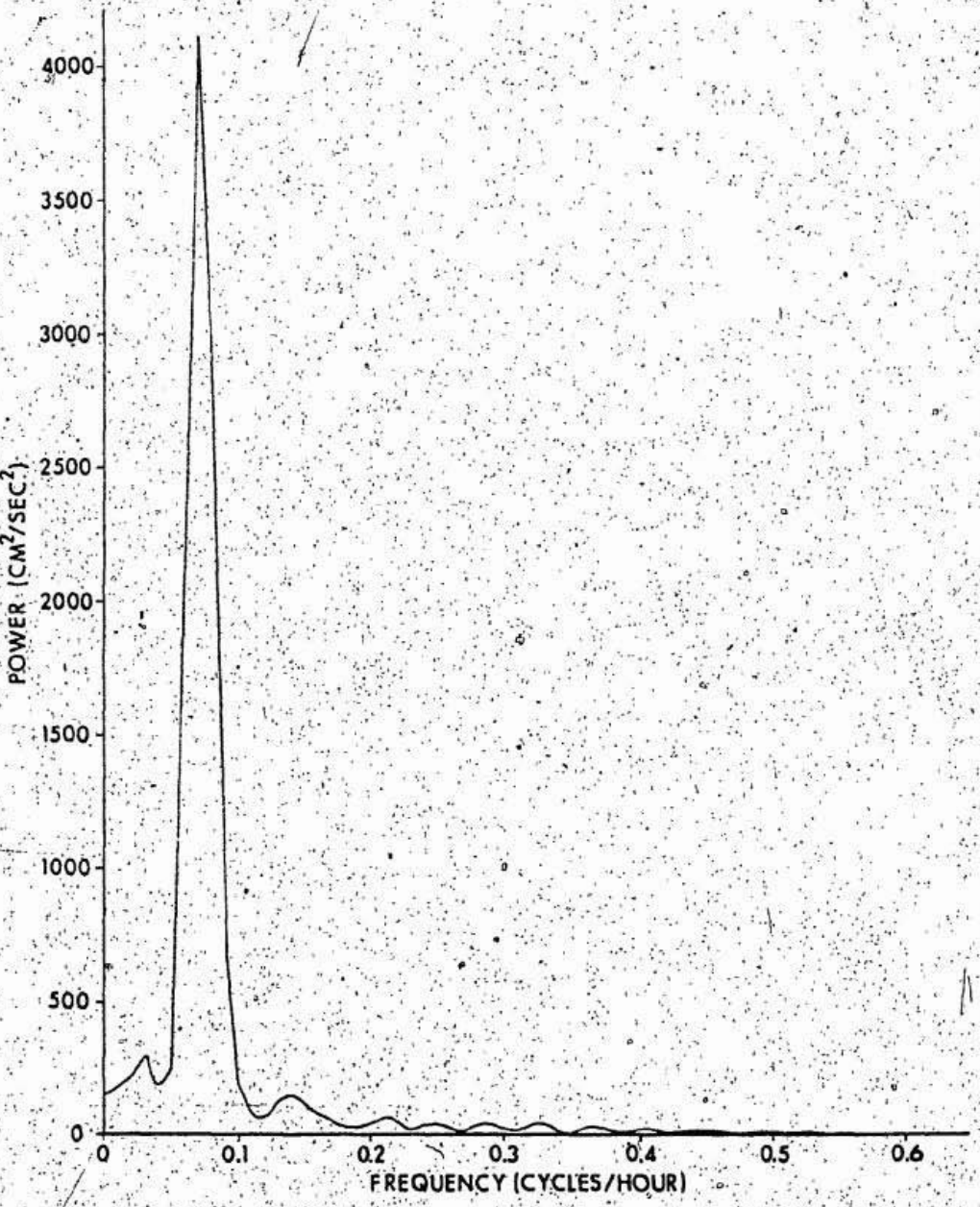

POWER SPECTRAL ESTIMATES
NORTH VELOCITY COMPONENT – METER C-1

Figure 8

of this value was used to summarize the cross-correlation between current records. In this study, this value is called the current meter cross-correlation parameter and is identified as r_c.

Of interest in section 5.6.4 is the relationship between r_c and d, the distance between two points. It is clear from the definition of $\gamma(\tau)$ that when d is equal to zero, $\gamma(\tau)$ becomes the autocovariance function of a current record. The maximum value for $\gamma(\tau)$ is one when d equals zero. Therefore, r_c is unity when d is equal to zero and the relationship between r_c and d must pass through the point (1, 0).

Only an approximation of the relationship between r_c and d was obtainable due to the few observations available. Various simple functional forms that met the above constraint and had desirable properties for weighting purposes (sec 5.6.3) were examined and the selected one is shown in Figure 9. The relationship has the form:

$$r_c^2 = 1 - d^2/a^2 \qquad (7)$$

r_c = current meter cross-correlation parameter

d = distance between points in miles

a = a constant

The constant a was evaluated by regressing d^2 on r_c^2 with the constraint that when d is equal to zero, r_c is equal to one. The best fit value for a was 14 miles.

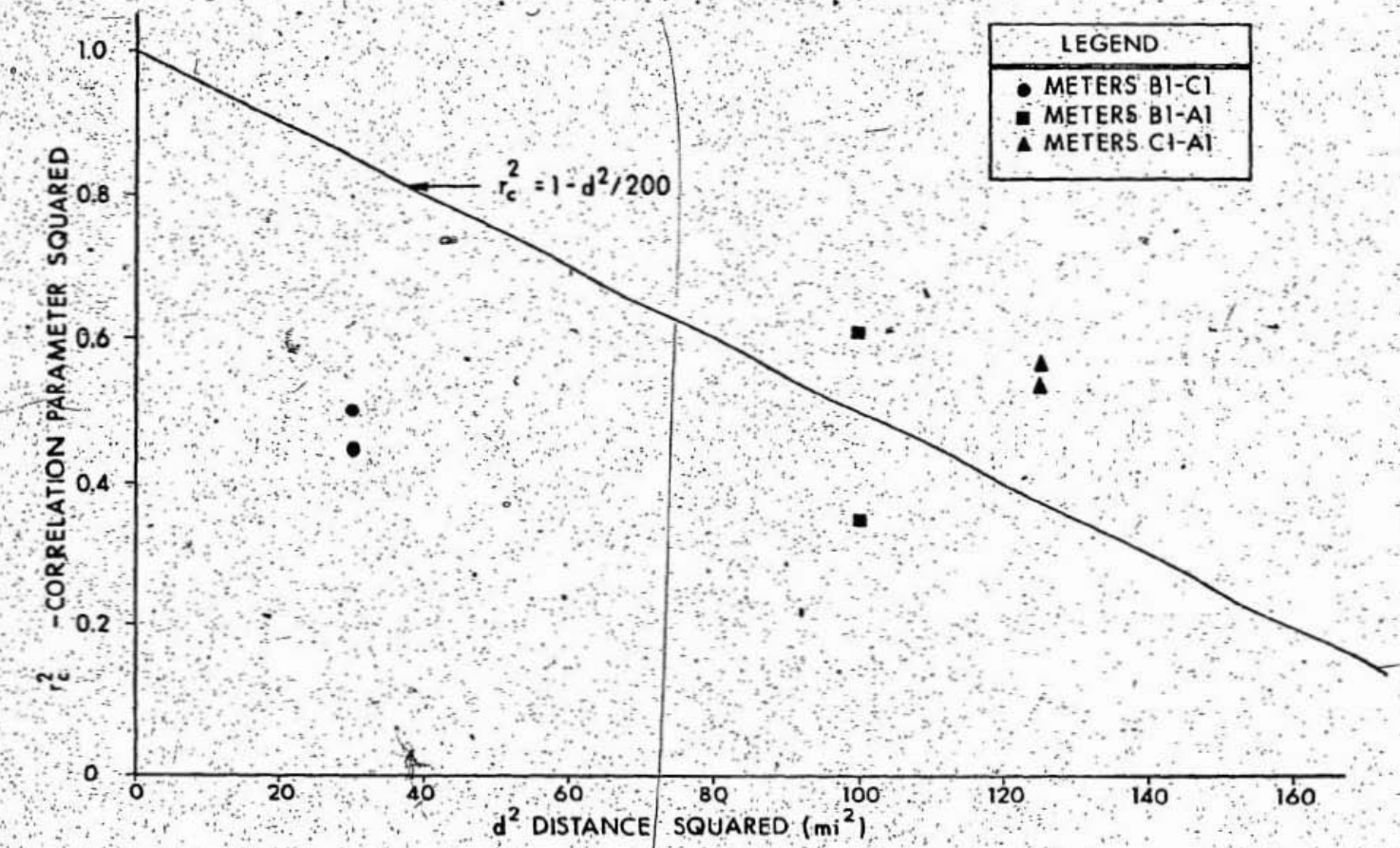

CURRENT METER CROSS-CORRELATION PARAMETER SQUARED
VS. DISTANCE SQUARED

Figure 9

To reduce the risk of using erroneous data a digital filter was applied to the data to remove as much experimental noise from the current records as possible. From Durdle (1969), the following fourth-order Butterworth filter was applied:

$$Y(nT) = .02608\ X\ (nT) + .10430\ X\ (nT-T) + .15647\ X\ (nT-2T) \quad (8)$$
$$+ .10430\ X\ (nT-3T) + .02608\ X\ (nT-4T) + 1.3066\ Y(nT-T)$$
$$- 1.0305\ Y(nT-2T) + .36240\ Y(nT-3T) - .05577\ Y(nT-4T)$$

The magnitude and phase response of this filter are shown in Figure 10.

The cut-off frequency for this filter is 3 times the Nyquist frequency, which is 1/2 the sampling rate. The sampling interval for the current meters was 20 minutes. Therefore the cut-off frequency is $3 \cdot (1/2) \cdot (1/3)$ per hour or 0.5 per hour, which is still twice the Nyquist frequency of 0.25 per hour for the iceberg data (sec 5.4). Thus, not only did the filter remove experimental noise, but there was no loss of useful information.

The filter is non-symmetric and it was, therefore, necessary to correct for a phase shift in the filtered signal. From Figure 10, the phase shift is approximately linear up to 120° at .4 cph. Therefore, the phase shift is approximately (120/360)/.4 hours or (2.5)/3 hours. Since the sample rate is 1/3 hours, this represents a shift of 2.5 sample intervals. Therefore, the filter output was advanced accordingly.

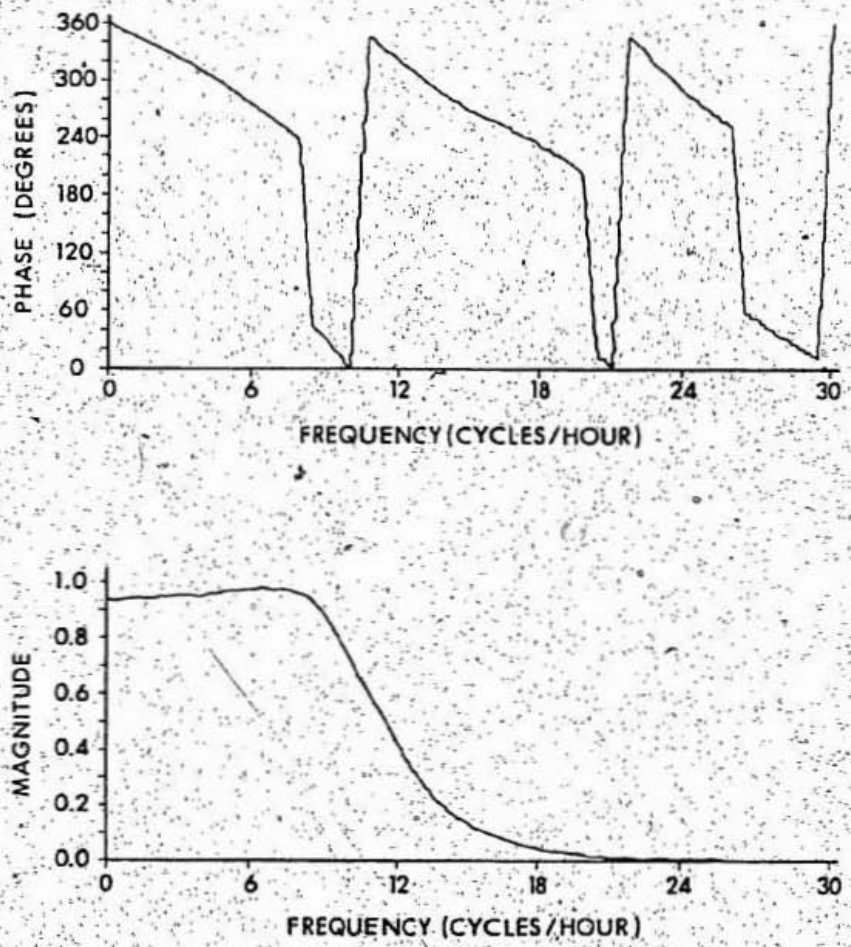

MAGNITUDE AND PHASE RESPONSE OF A 4TH. ORDER BUTTERWORTH DIGITAL FILTER WITH CUT-OFF AT 10 CYCLES/HOUR (after Durdle, 1969).

Figure 10

The filtering procedure was applied to both the N-S and E-W components of current meters A1, B1, and C1.

5.3 Wind Data

No continuous record of wind was made at the sea surface. However, observations were made hourly at the Saglek shore station and approximately every four hours aboard the C.S.S. Dawson. Fifty-seven pairs of observations were available. To estimate the time series of the wind velocities being experienced by the icebergs in the study area, which was assumed to be the same as that measured on board the Dawson, the two sets of data were extracted from field notes and the log of the Dawson (Bedford Institute of Oceanography, 1972) and correlations between components of the wind vectors were examined. The following best fit equations were derived:

$$D_n = -.334 + .526\ S_n - .018\ S_e; \quad r = .543 \qquad (9)$$

$$D_e = -2.03 - .379\ S_n + 1.04\ S_e; \quad r = .802$$

D_n = north component of Dawson wind observation

D_e = east component of Dawson wind observation

S_n = north component of Saglek wind observation

S_e = east component of Saglek wind observation

r = coefficient of multiple correlation

Using the interpretation techniques outlined in Section 7.2, the Dawson observations were, on the average, .83 of the speed and 13°

counterclockwise of the Saglek data. Saglek is at elevation 1800 feet whereas the Dawson's measurements were made near sea level. Thus the measurements represent observations at different heights in the atmospheric friction layer. After Haltiner and Martin (1957), a spiral similar to the well-known Ekman spiral for ocean currents (Neumann and Pierson, 1966) exists in a wind layer. At the top of the layer, the wind is geostrophic and at the bottom it is given by:

$$V_o = V_g (\cos\chi_o - \sin\chi_o) \qquad (10)$$

V_o = wind speed at bottom layer

V_g = geostrophic wind

χ_o = angle (counterclockwise) from geostrophic wind to V_o

The value 13° is within the range they report for χ_o, which predicts a corresponding value of .75 for V_o/V_g. The observed thirteen degrees is, therefore, probably low which indicates that the Saglek winds were not completely on the top of the friction layer. However, the results of the comparison of the two sets of data are plausible. This consideration, combined with the satisfactory coefficients of multiple correlation (both are significant at 90% confidence levels) associated with equation (9), supported the acceptance of equation (9) as valid and the Saglek data were used with equation (9) to estimate sea surface conditions.

Where gaps in the data still existed, linear interpolation of the vectors with respect to time was used to estimate the missing information.

The winds during the study were generally light. The 57 observations used in the cross-correlation study were scattered throughout the period. At Saglek, they averaged 8.5 kts from the southwest with a maximum of 50 kts from the southwest and on board the Dawson they averaged 6.1 kts from the west with a maximum of 50 kts from the west.

5.4 Iceberg Data

Iceberg movements were recorded by a crew at Saglek, Labrador from a large radar screen with a range of about 50 miles. As an iceberg was identified, it was assigned a code name indicating the date in August 1972 and the order on the day that it was sighted. For example, Berg 10E was first sighted on the tenth of August and was the fifth iceberg, indicated by E, sighted on that day. Approximately every 2 hours, the range and bearing of all icebergs on the screen were recorded. Sample trajectories are shown in Figure 4.

At the end of the study, the ranges and bearings were converted to rectangular Cartesian co-ordinates in nautical miles. Saglek was assigned the co-ordinates (16,50) to ensure all iceberg positions had positive co-ordinates and the X-axis was oriented in an east-west direction with east positive and the Y-axis oriented in a north-south direction with north positive. The distance of each sighting from the position of the current meter strings was also calculated.

Finally, the components of each iceberg's velocity vectors were calculated, as well as their possible range due to measurement

error. The radar screen could be read to the nearest ±0.5 degree and ±0.5 mile. Thus every reading located an iceberg within a sector of an annulus of the region (Figure 11). To estimate the error in the calculation of velocity, the fastest and slowest possible velocities were calculated. These results were used to weight the observations (sec 5.6.3).

5.5 Selection of Data for Analysis

5.5.1 Introduction

This section describes the manner in which data were selected for analysis.

5.5.2 Distance between Icebergs and Current Meters

The spatial variation in current limited the icebergs which could be used in the analysis. After Dempster (1973), Figure 4 indicates the variation in currents in the study area. Clearly, a direct measurement of current is representative of only a limited area, and if successful correlations with iceberg behaviour are to be achieved, some maximum allowable distance between an iceberg and a current meter must be specified.

Ten miles was used to limit the data which were analyzed. In practice this is the distance where icebergs are monitored during a

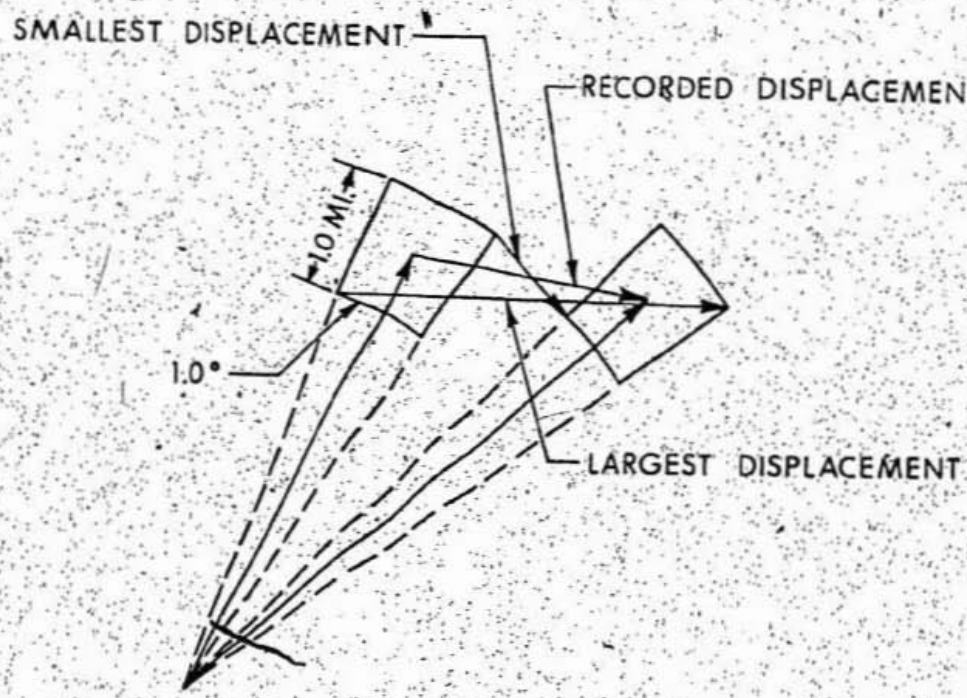

IMPACT OF MEASUREMENT ERROR ON
DISPLACEMENT ESTIMATION

Figure 11

drilling operation (Ainslie, 1974). Also, from section 5.2 equation (7), the current cross-correlation parameter r_c has a satisfactory value of about .7 at a distance of 10 miles.

5.5.3 Number of Iceberg Observations

The minumum number of iceberg observations necessary before an iceberg could be included in the analysis was set at 9, based on a balance of the number of observations required to estimate the model parameters for an individual iceberg and the number of icebergs required to permit general interpretation of the model parameters. The correlation model (chapter 3) has 5 regression coefficients for each velocity component, therefore 6 observations represents an absolute minimum number required. The limit of 9 observations was chosen giving 4 degrees of freedom and leaving 33 icebergs suitable for analysis. Since a sample of 30 is commonly considered statistically "large", this provided a satisfactory basis for generalization. The number of sightings of individual icebergs ranged from 9 to 53, with a mean value of 21 (Table 1).

5.5.4 Selection of Environmental Data

Each pair of iceberg sightings which met the criteria outlined in sections 5.5.2 and 5.5.3 was converted to an average iceberg velocity vector to form one of the observations of the dependent variables in the regression analysis (chapter 3). To provide the corresponding inde-

TABLE 1

GENERAL INFORMATION FOR 33 ICEBERGS AVAILABLE FOR STUDY

Iceberg	Current Meter	Start Time (ADT)	Start Day Aug. 1972	End Time (ADT)	End Day Aug. 1972	Number of Observations
7L	A1	250	13	1710	20	53
7M	A1	100	12	920	16	22
10A	A1	2335	13	320	19	40
10E	A1	100	12	2330	13	9
11S	A1	250	13	2115	15	16
14D	A1	1635	14	315	17	21
17B	A1	905	22	1515	23	13
17D	A1	105	22	1515	23	18
19B	A1	320	20	1515	22	20
20C	A1	940	20	915	22	20
20D	A1	940	20	1150	22	20
21B	A1	1145	22	1515	23	14
7L	B1	115	18	2320	20	27
8F	B1	100	12	800	14	9
11G	B1	255	13	1740	15	16
11R	B1	100	12	810	14	10
12C	B1	1705	14	305	16	14
13A	B1	520	14	2125	15	17
13B	B1	1715	14	40	17	12
13G	B1	700	16	2310	19	31
14A	B1	1900	14	1625	17	24
17A	B1	2300	17	1705	19	18
18A	B1	1520	19	1900	20	11
7L	C1	100	12	2100	19	49
7M	C1	100	12	2125	14	11
10A	C1	255	13	1625	17	29
11G	C1	255	13	110	15	11
11R	C1	100	12	1010	14	11
13G	C1	510	17	1300	18	13
17B	C1	1905	19	120	23	28
17D	C1	1325	17	115	23	47
20B	C1	1145	22	1505	23	14
21B	C1	2130	21	1515	23	21

pendent variables, the wind and current records were averaged during the same time intervals lagged by various trial time lags t_c and t_w respectively.

5.6 Weighting of Observations

5.6.1 Introduction

The reliability of an individual iceberg observation for estimating the correlation model parameters varies considerably. It is essential, therefore, that the observations be weighted accordingly, prior to estimating the parameters. The method of analysis was modified following Smillie (1966) to allow weighting of the observations. In essence, this involved multiplying both the LHS and RHS of equations (3a) and (3b) by appropriate weighting factors prior to conducting the least squares fit. The following paragraphs describe the development of the weighting factors which were used in this study. It was assumed that the functional details of the factors are of little importance, provided they reasonably reflect the relative reliability of the observations used.

5.6.2 Differences in Time between Iceberg Sightings

During collection of the iceberg drift data at Saglek, it was impractical to record iceberg positions at precisely regular intervals. Sometimes an iceberg would be missing from the radar screen for a short time, and many times the volume of data to be recorded from the screen

or equivalent problems caused a delay in an iceberg's position being noted. In general, however, observations were made every 2 to 4 hours.

This variation was accounted for by weighting each observation by multiplying it by the length of time between iceberg sightings. Since the terms in equations (3a) and (3b) are velocity terms, they were effectively converted to displacement terms, and the objective function to be minimized, σ^2, by the regression analysis became effectively the sum of the squares of the magnitude of the unexplained berg displacements.

5.6.3 Variations in Accuracy of Iceberg Data

The accuracy with which an iceberg could be located depended on its position on the radar screen. Range could be measured to ± 0.5 miles and bearing to ± 0.5 degrees. Thus an iceberg was in fact located within a sector of an annulus, which increased in size, the farther the iceberg was from the centre of the radar field. When two observations were compared to estimate displacement, considerable variation was possible (Figure 11).

To allow for this variation, weighting factors W_{bx} and W_{by} were used:

$$W_{b_x} = \exp-(\Delta b_x/v)^2 \qquad (11)$$

$$W_{b_y} = \exp-(\Delta b_y/v)^2 \qquad (12)$$

Δb_x = maximum absolute error in the x-component of ice berg velocity

Δb_y = maximum absolute error in the y-component of iceberg velocity

v = a factor which controls sensitively of the weighting factor.

The functional form of the weighting factors, $\exp(-U^2)$, was selected because it had a value 1.0 for complete certainty (U=0) and because its slope is flat near the region of complete certainty. The factors are functions of the absolute velocity error, rather than relative velocity error, in order that the factors only reflect variations in accuracy due to position on the radar screen. The sensitivity factor, v, was selected at 10cm/sec, which is near the upper limit of the errors encountered. Therefore, for example, when Δb_x or Δb_y equals 10 cm/sec, W_{b_x} and W_{b_y} have values of 0.37.

5.6.4 Distance between Iceberg Sightings and Current Meters

The degree to which a current meter can be expected to contribute to explaining an iceberg's motion can be expected to decline as the distance between the current meter and the iceberg increases. This is due to the observed drop in cross-correlation between current records with distance (section 5.2). For this reason, additional weighting factors, similar to those introduced in section 5.6.3 were used:

$$W_{d_x} = \exp-(d_x/d_o)^2 \quad (13)$$

$$W_{d_y} = \exp-(d_y/d_o)^2 \quad (14)$$

d_x = distance, in the x-direction, between current meter and iceberg

d_y = distance, in the y-direction, between current meter and iceberg

d_o = a sensitivity factor

The factor d_o was chosen from the relationship between the current cross-correlation parameter and distance (see Figure 9). For this study it had the value of 14.1 nautical miles, which is the square root of 200 nautical square miles.

5.6.5 Combined Weighting Factors

Combining the above factors gives the weighting factors used:

$$W_{xi} = \Delta t_i \exp(-d_{xi}^2/200 - \Delta b_{xi}^2/100) \quad (15)$$

$$W_{yi} = \Delta t_i \exp(-d_{yi}^2/200 - \Delta b_{yi}^2/100) \quad (16)$$

i = observation number

W_{xi} = weighting factor in the x direction

W_{yi} = weighting factor in the y direction

Δt_i = time between sightings

d_{xi} = iceberg distance from current meter in nautical miles, x direction

d_{yi} = iceberg distance from current meter in nautical miles, y direction

Δb_{xi} = maximum error in iceberg velocity in cm/sec, x direction

Δb_{yi} = maximum error in iceberg velocity in cm/sec, y direction

6. RESULTS

Following the procedures outlined in chapter 3, the data for the 33 acceptable icebergs were used to estimated the regression coefficients for equations (3a) and (3b) and to select the optimum values for wind lag time, t_w, and current lag time, t_c. The results are presented in Table 2. For Iceberg 10E, the estimated and actual north and east velocity components are plotted in Figures 12 and 13 and the corresponding trajectory is shown in Figure 14.

No formal method was developed in this study to evaluate the statistical significance of the results, however, some indication of the comparative success or failure of the application of equations (3a) and (3b) was obtained using:

$$r_m = \left[1 - \left[\frac{\sum_{i=1}^{N} |\underline{W}_i \cdot \underline{e}_i|^2}{\sum_{i=1}^{N} |\underline{W}_i \cdot \underline{b}_i|^2} \right] \right]^{1/2}$$

r_m = model reliability factor

$\underline{W}_i$ = vector containing W_{xi} and W_{yi}, the ith weighting factors

$\underline{e}_i$ = ith vector residual

$\underline{b}_i$ = ith iceberg velocity vector

N = number of a observed velocity vectors for an iceberg

This parameter has some similarity to a scalar multiple correlation coefficient. When r_m is equal to one, the model used is

TABLE 2

ESTIMATED ICEBERG CROSS-CORRELATION PARAMETERS

Iceberg	Current Meter	Constant Vector r_x (cm/sec)	r_y (cm/sec)	Current Transformation P_{11}	P_{12}	P_{21}	P_{22}	Optimum Current Time Lag (Min). t_c
7L	A1	-4.58	-.690	-.403	.171	.345	-.105	360
7M	A1	.642	.258	-.254	.000	-.542	.721	160
10A	A1	-4.13	-10.4	.022	.148	-.075	-.047	360
10E	A1	15.1	1.50	-1.69	2.14	-.593	.342	260
11S	A1	-9.65	-5.60	-.583	1.08	-.960	.238	200
14D	A1	-19.2	-4.64	-.473	-.130	-.092	-.217	340
17B	A1	-10.8	-16.3	-.319	-.086	.091	.312	0
17D	A1	-3.79	-30.5	-.155	.278	-.218	-.128	320
19B	A1	-3.87	-5.00	-.060	.230	-.225	-.092	340
20C	A1	-7.11	-4.64	-.416	.022	-.229	-.065	220
20D	A1	-7.81	-10.8	-.267	.001	-.126	.200	240
21B	A1	3.09	-16.0	-.162	.105	-.296	-.365	320
7L	B1	-2.63	-7.64	.071	-.003	-.394	.304	0
8F	B1	21.5	-4.79	-1.17	.368	.878	2.29	80
11G	B1	-3.63	-10.1	-.054	-1.20	.069	.558	80
11R	B1	12.2	.745	-1.40	-.094	-.570	.715	180
12C	B1	10.8	-21.9	1.53	-.528	.221	.635	100
13A	B1	2.76	-13.4	-.551	.805	.847	-.141	360
13B	B1	-8.57	-14.0	.141	-1.33	-.424	.642	40
13G	B1	-.905	-9.65	-.122	.264	.742	.107	320
14A	B1	-.416	-15.9	.071	-.643	.370	.800	80
17A	B1	11.2	-23.4	-1.96	-.074	.241	.414	220
18A	B1	-16.3	-13.4	-.803	-1.26	.578	1.33	320
7L	C1	-5.05	.389	.268	-.340	-.350	.501	0
7M	C1	3.87	-7.02	.706	-.152	.669	.129	160
10A	C1	-9.18	-12.2	.072	-.227	-.202	.116	360
11G	C1	-24.8	-22.9	-.287	-1.66	.168	-.429	280
11R	C1	8.75	5.41	-.389	.144	.795	.496	160
13G	C1	-6.04	.069	.162	-.168	-.112	.122	60
17B	C1	.865	-3.77	-.077	.123	-.187	.000	140
17D	C1	-2.19	3.25	-.262	.115	.023	-.092	360
20B	C1	-1.23	-15.3	.207	.017	-.317	.016	180
21B	C1	-20.5	-28.6	-.259	.065	-.062	-.241	360

TABLE 2 (cont'd)

ESTIMATED ICEBERG CROSS-CORRELATION PARAMETERS

Iceberg	Current Meter	Wind Transformation q_{11} (%)	q_{12} (%)	q_{21} (%)	q_{22} (%)	Optimum Wind Time Lag (min) t_c	Model Reliability Factor r_m
7L	A1	.644	.194	-.573	1.27	200	.483
7M	A1	.543	.817	-.744	.006	200	.898
10A	A1	.302	-.037	.345	.681	300	.495
10E	A1	-3.86	-8.27	5.99	2.82	300	.984
11S	A1	.822	7.15	-.619	-1.57	180	.673
14D	A1	-.308	5.02	-.249	-2.28	240	.835
17B	A1	.416	.670	-.106	-.296	260	.784
17D	A1	.713	.855	.139	.179	260	.829
19B	A1	.568	.036	-.374	1.15	220	.917
20C	A1	.362	-.041	-.683	.625	140	.733
20D	A1	.549	.088	.098	1.43	60	.700
21B	A1	-.641	-1.18	-.541	-2.14	240	.000
7L	B1	.166	-.023	-.518	1.11	60	.581
8F	B1	4.54	1.80	.256	-2.12	200	.892
11G	B1	.847	1.06	-.368	.500	300	.774
11R	B1	3.01	2.37	2.08	-.106	360	.908
12C	B1	-.094	3.17	-.136	-.932	280	.975
13A	B1	.173	2.50	.099	-2.37	280	.915
13B	B1	.406	1.88	.502	.103	160	.800
13G	B1	.634	.325	.663	1.11	140	.900
14A	B1	.435	-.241	.398	.567	0	.867
17A	B1	3.43	1.32	-.162	.024	320	.934
18A	B1	2.45	-1.43	-.226	5.08	180	.932
7L	C1	.778	.293	-.635	.493	280	.547
7M	C1	1.09	1.50	-1.14	-1.08	280	.726
10A	C1	.447	-.283	.354	1.40	260	.756
11G	C1	-3.34	2.82	-2.21	3.05	360	.775
11R	C1	2.41	-.594	2.90	-.307	280	.756
13G	C1	2.60	1.04	-4.42	-1.46	260	.973
17B	C1	.333	-.061	-.673	.858	180	.725
17D	C1	.636	.359	-1.24	-.351	100	.843
20B	C1	-.916	-1.75	-4.02	.766	0	.944
21B	C1	1.00	.125	.711	.467	20	.102

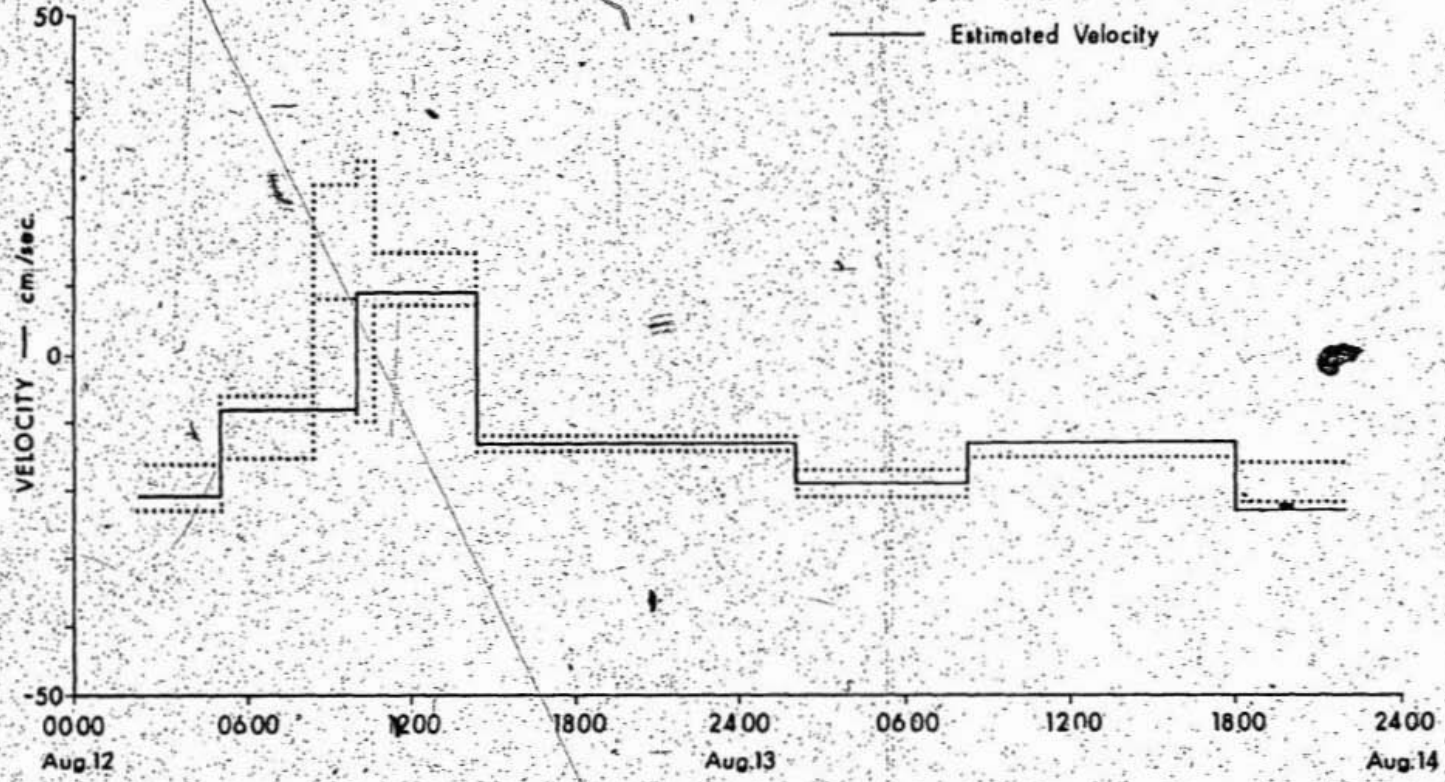

BERG 10E — MEASURED AND ESTIMATED NORTH VELOCITY.

Figure 12

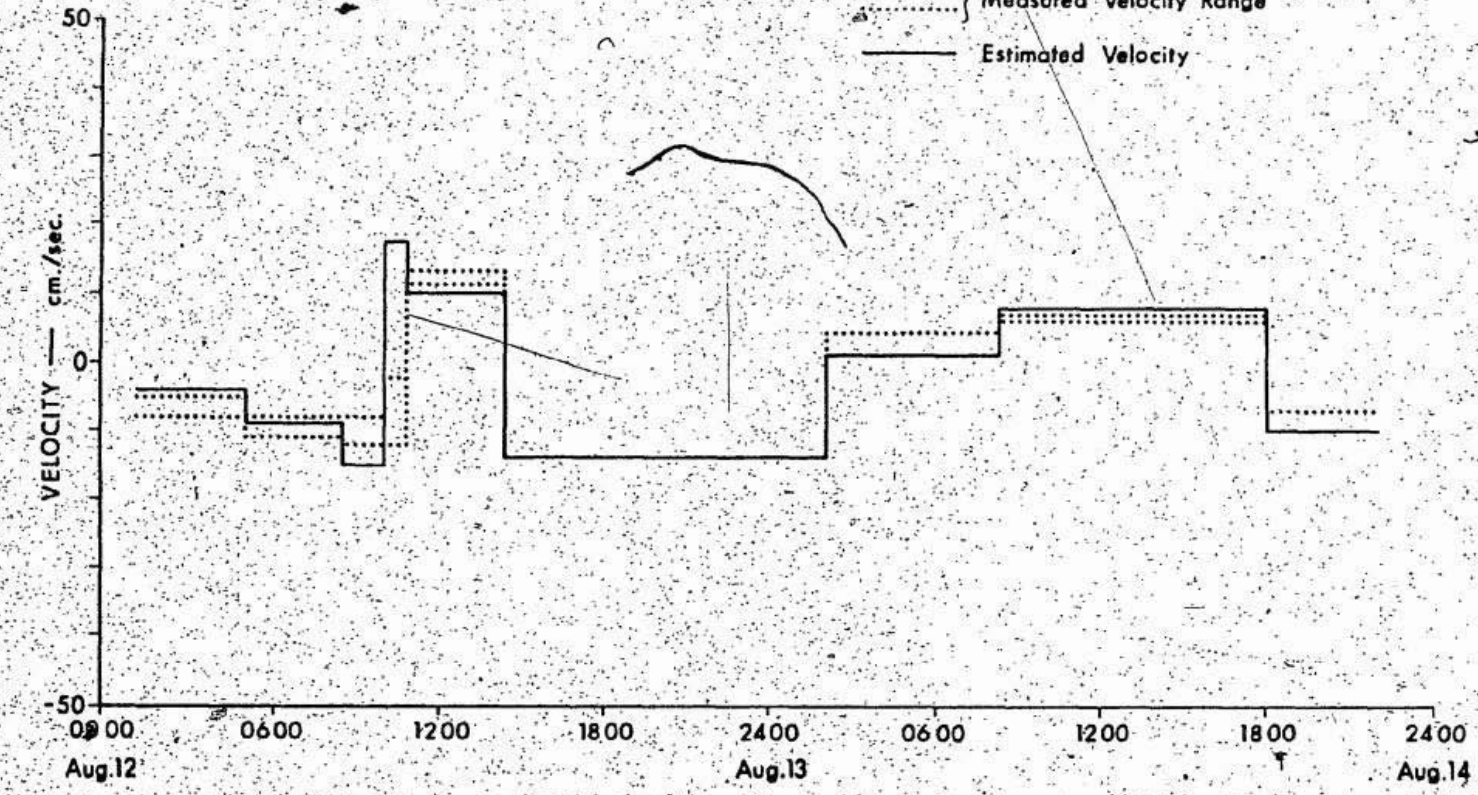

BERG 10E — MEASURED AND ESTIMATED EAST VELOCITY.

Figure. 13

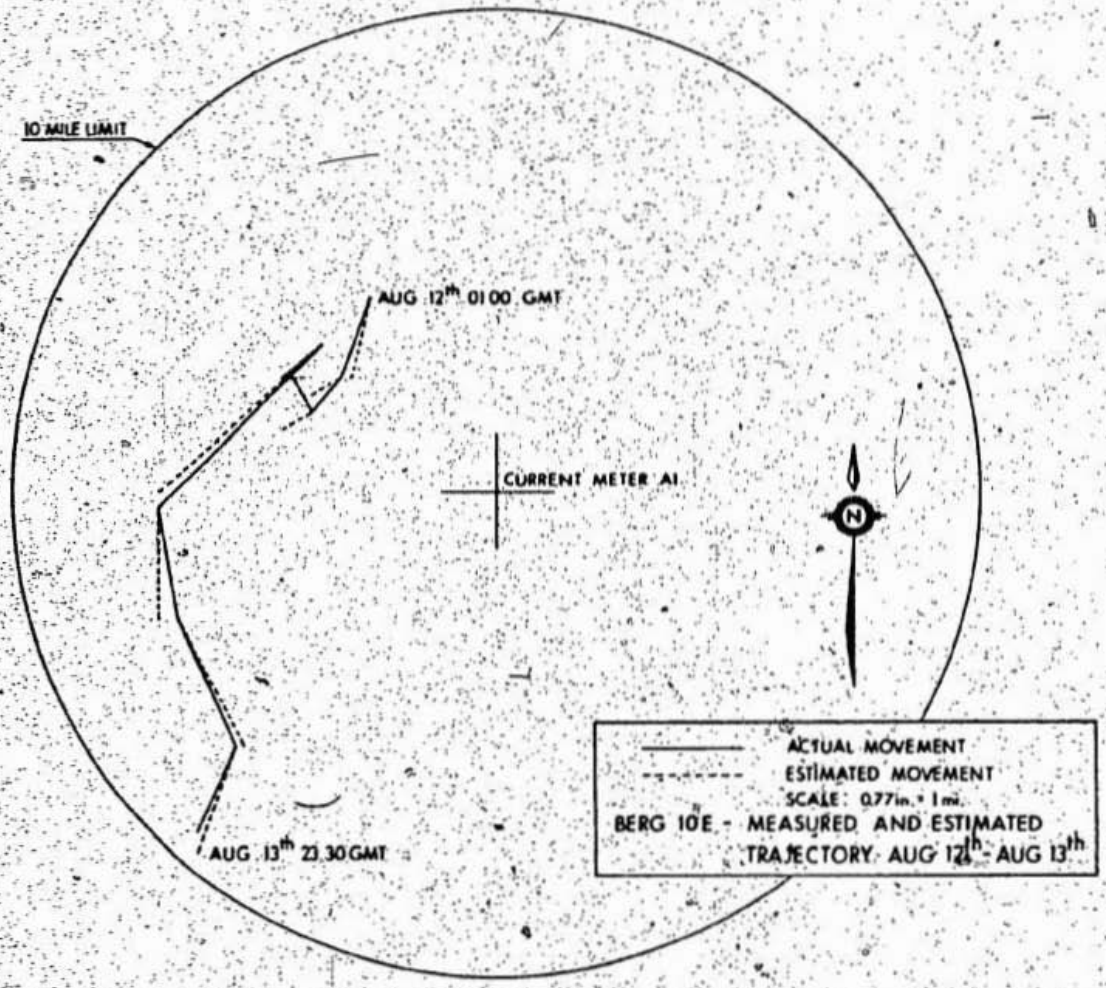
10 MILE LIMIT
AUG 12th 0100 GMT
CURRENT METER A1
N
AUG 13th 2130 GMT
ACTUAL MOVEMENT
ESTIMATED MOVEMENT
SCALE: 0.77in. = 1mi.
BERG 10E - MEASURED AND ESTIMATED TRAJECTORY AUG 12th - AUG 13th

Figure 14

perfect, and the smaller r_m becomes the less successful is the model. It is evident that, as the objective function O^2 (chapter 2) increases, r_m decreases.

Because $\underline{W}_i \cdot \underline{e}_i$ and $\underline{W}_i \cdot \underline{b}_i$ can also be considered weighted displacements (sec 5.6.2), $(1 - r_m^2)$ can be considered to represent the weighted ratio of the sum of the squares of an iceberg's unexplained displacement to the sum of the squares of its observed displacement.

7. INTERPRETATION OF RESULTS

7.1 Introduction

The purpose of this chapter is to verify the transfer functions obtained for the cross-correlation model of chapter 3 by showing they are reasonably consistent with theory and observation. First, the model must be rearranged to a form which can be readily interpreted. This rearrangement is based on a discussion of iceberg dynamics.

7.2 Iceberg Dynamics and Transformation of the Cross-Correlation Model

An iceberg can be considered a free body moving at the interface of two unsteady, non-uniform fluids. The forces acting on an iceberg are due to:

gravity

pressure gradients

wind drag

wind lift

water drag

water lift

waves and swell

Coriolis effects

Since the concern of this study is the horizontal movement of icebergs, only the horizontal components of these forces need be considered. Thus, gravity and vertical pressure gradients can be ignored. Horizontal pressure gradients, waves and swell forces are generally small and can also be ignored. Wind and water lift depend on the shape and orientation of an iceberg. Since neither of these data are generally available, the forces were necessarily treated as random and unknown. They will generally be negligible unless a berg has a unusually aerodynamic shape. Thus, an iceberg's horizontal motion is largely determined by:

wind drag

water drag

Coriolis forces

Ideally, therefore, the majority of an iceberg's motion could be explained by understanding the iceberg's interaction with the air and the sea. Unfortunately, each of these has a velocity field which is extremely complex and interrelated with the other. Even if an iceberg's response to wind or current could be described theoretically, there is unlikely to be adequate detailed knowledge of local wind and current fields for application of such results to iceberg movement.

If it is assumed, however, that the complex dynamics can be approximated by simple transformations of representative wind and current vectors, it is possible to construct a model, containing the essential characteristics of iceberg dynamics, which can be related to the model postulated in chapter 3.

First, it is assumed that if an iceberg were moving in a uniform, unsteady current, the iceberg velocity would be the sum of the mean current velocity and some transformation of the unsteady or transitory component of the current. That is,

$$\hat{\underline{b}} = \bar{\underline{c}} + A[\underline{c} - \bar{\underline{c}}] \qquad (17)$$

$\hat{\underline{b}}$ = estimated iceberg velocity vector

$\underline{c}$ = current velocity vector

$\bar{\underline{c}}$ = mean current velocity

A = transformation matrix

Any current field is, however, non-uniform and any current measurement only samples a few points in the field. In addition, the shape of an iceberg is generally irregular and therefore, a second transformation is introduced to convert an observed current vector to the effective current experienced by an iceberg. Finally, a third transformation is required to account for the influence of wind on iceberg movement. The complete model, then, has the form:

$$\hat{\underline{b}} = T\,[\,\bar{\underline{c}} + A\,(\underline{c} - \bar{\underline{c}})\,] + Q\underline{w} \qquad (18)$$

T = current averaging matrix

$\underline{w}$ = wind vector

Q = wind transformation matrix

which simplifies to:

$$\hat{\underline{b}} = \underline{r} + P\underline{c} + Q\underline{w} \qquad (19)$$

$$\underline{r} = T(I-A)\underline{c} \quad (19a)$$

$$P = TA \quad (19b)$$

and in scalar form becomes:

$$\hat{b}_x = r_1 + p_{11}c_x + p_{12}c_y + q_{11}w_x + q_{12}w_y \quad (20a)$$

$$\hat{b}_y = r_2 + p_{21}c_x + p_{22}c_y + q_{21}w_x + q_{22}w_y \quad (20b)$$

which can be compared with equations (3a) and (3b).

To interpret the regression coefficients in equations (3a) and (3b), $\underline{r}$, P, and Q were first reduced to the matrices T, A, and Q. By calculating $\underline{c}$ during the period of comparison and assuming T to be a linear transformation involving only rotation and magnification, equation (19a) was solved for the elements of T and subsequently equation (19b) was solved for the elements of A. The matrix Q did not require manipulation.

Secondly the effect of the transformations on the vectors on which they operate was summarized by applying each one to a unit vector. The unit vector was rotated through 360° and its average change in magnitude and direction caused by each transformation was calculated. The results are summarized in Table 3 for the 33 icebergs studied.

7.3 Summary of Observed Characteristics of Iceberg Motion

The estimated iceberg responses are summarized in Table 4.

TABLE 3

ESTIMATED ICEBERG RESPONSES

Iceberg	Current Meter	Mean Current Magnitude	Mean Current Direction[1]	Rotary Current Amplitude	Rotary Current Phase[1]	Rotary Current TimeLag[2]	Wind Magnitude[3]	Wind Direction[1]	Wind TimeLag[2]
7L	A1	0.336	-54.8	1.078	-32.0	360	2.07	-21.9	200
7M	A1	0.552	25.8	1.117	-37.7	160	1.68	-71.0	200
10A	A1	0.955	-17.1	0.123	-79.3	360	1.08	21.2	300
10E	A1	0.575	-67.1	3.138	-49.2	260	14.8	94.1	300
11S	A1	1.572	-61.4	0.684	-38.2	200	9.18	-95.5	180
14D	A1	1.006	-74.2	0.365	-109.0	340	6.88	-116.2	240
17B	A1	1.103	-20.6	0.297	36.3	0	1.06	-58.6	260
17D	A1	1.453	-9.0	0.197	-110.6	320	1.45	-32.9	260
19B	A1	0.479	-63.5	0.502	-45.1	340	1.77	-13.5	220
20C	A1	0.472	-50.5	0.659	-101.9	220	1.27	-33.1	140
20D	A1	1.073	-26.3	0.231	-17.8	240	2.03	0.3	60
21B	A1	0.357	6.7	0.968	-149.5	320	3.24	19.1	240
7L	B1	2.142	12.4	0.150	-58.6	0	1.55	-21.3	60
8F	B1	4.279	34.7	0.433	5.9	80	7.06	-13.8	200
11G	B1	2.946	32.7	0.286	35.6	80	1.99	-46.7	300
11R	B1	1.932	49.6	0.595	4.8	180	5.67	-4.0	360
12C	B1	7.174	67.9	0.166	-48.8	100	4.11	-107.2	280
13A	B1	4.119	64.8	0.215	22.2	360	4.28	-41.4	280
13B	B1	5.689	31.9	0.178	11.1	40	2.56	-34.3	160
13G	B1	3.407	22.1	0.160	25.7	320	1.89	11.0	140
14A	B1	6.658	67.6	0.109	-18.3	80	1.16	32.5	0
17A	B1	8.992	52.5	0.147	36.4	220	4.56	-23.2	320
18A	B1	4.823	-3.9	0.277	56.7	320	7.73	9.1	180
7L	C1	0.500	-31.8	0.957	30.7	0	1.57	-36.7	280
7M	C1	1.319	41.8	0.494	2.7	160	3.33	-50.6	280
10A	C1	1.627	5.7	0.139	1.4	360	2.01	19.1	260
11G	C1	3.276	14.0	0.346	97.3	280	7.25	-52.4	360
11R	C1	1.004	103.8	0.685	-11.5	160	4.76	59.0	280
13G	C1	0.320	-75.9	0.571	87.0	60	6.73	-78.3	260
17B	C1	0.473	-36.9	0.345	-39.2	140	1.45	-27.2	180
17D	C1	0.552	-151.9	0.362	-13.4	360	1.85	-79.9	100
20B	C1	0.968	41.8	0.251	-98.0	180	2.82	28.9	0
21B	C1	2.067	-29.7	0.125	-136.1	360	1.69	21.7	20

[1]degrees counterclockwise [2]minutes [3]percent

TABLE 4

WEIGHTED MEANS OF ESTIMATED BERG RESPONSES

PARAMETER	UNITS	WEIGHTED MEAN	STANDARD ERROR OF THE MEAN	MINIMUM	MAXIMUM
MAGNITUDE RELATIVE TO MEAN CURRENT	-	2.46	0.36	0.32	9.0
DIRECTION RELATIVE TO MEAN CURRENT	deg (1)	-0.83	8.62	-152	104
AMPLITUDE RELATIVE TO ROTARY CURRENT	-	0.499	0.09	0.109	3.14
PHASE ANGLE RELATIVE TO ROTARY CURRENT	deg (1)	-13.7	8.31	-150	97
MAGNITUDE RELATIVE TO WIND SPEED	%	3.99	.49	1.06	14.8
DIRECTION RELATIVE TO WIND (2)	deg (1)	-25.0	7.40	-116	94
BEST CORRELATION TIME LAG - CURRENT	minutes	204	18	0.0	>360
BEST CORRELATION TIME LAG - WIND	minutes	214	15	0.0	>360
VECTOR CORRELATION COEFFICIENT (3)	-	.822	.02	0.0	0.984

NOTES:

(1) DEGREES COUNTERCLOCKWISE

(2) AT STEADY STATE

(3) EQUIVALENT TO A SCALAR CORRELATION COEFFICIENT - CAN BE INTERPRETED AS AVERAGE FRACTION OF MEASURED TRAJECTORY EXPLAINED FOR EACH BERG.

(4) NO. OF BERGS STUDIED - 33

(5) $\sqrt{33} = 5.745$

The first two rows of Table 4 refer to the matrix T, which operates on the mean current vector, the third and fourth row to the matrix A which is the response to the transitory current, and the fifth and sixth row to the matrix Q, the response to wind.

The characteristics are summarized by a weighted mean calculated using the model reliability factor, r_m (chapter 6). This coefficient was also averaged and the value is also recorded in Table 4. The average value of .822 indicates that (chapter 6), on the average a 20% error can be expected when an icebergs movement is modelled using cross-correlation with wind and current data (see Figure 15).

It appears that the icebergs studied moved generally 2.5 time faster than the mean current as measured by the surface current meters used in the study during the observation of each iceberg. Considering the vertical shear in the currents in the region identified by Holden (1974), and that the surface current meters used in the analysis were at a depth of 13 m, it is not surprising that the effective steady current experienced by the icebergs was higher than measured. The icebergs moved, however, in approximately the direction of the mean currents, which supports the assumption used, for example, by Dempster (1974) that Coriolis drift, relative to a steady current, is negligible.

The icebergs significantly dampened the effect of the transitory component of the current. Because of the considerable variation in the transitory current component, the response was also highly

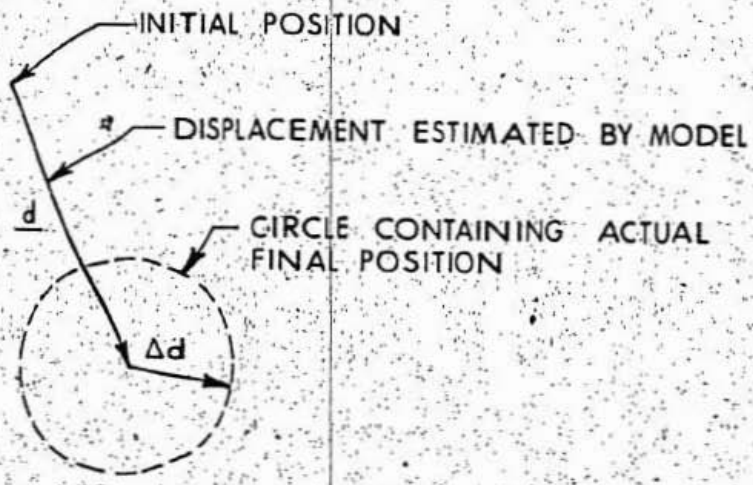

$$\frac{\Delta d^2}{d^2} = .17$$

$$1 - \frac{\Delta d^2}{d^2} = .822$$

INTERPRETATION OF MODEL RELIABILITY FACTOR

Figure 15

variable. On average, iceberg velocities showed only .499 of the amplitude of the current meters and the velocity vectors were 13.7 degrees clockwise of the transitory components of the current meter records. Since the iceberg vectors correlated best with current vectors 204 min (3.4 hrs) earlier, the phase shift of 13.7 deg. must be adjusted. According to the power spectrum of the current records, the transitory currents had an average period of about 13.7 hrs. Thus 3.4 hrs represents .25 of a cycle, or 90 deg. From Figure 7, the predominant rotation of the transitory current was clockwise. Therefore, the iceberg velocity vectors were trailing the current vectors by 76.3 degrees.

From Appendix A, an iceberg's amplitude response and phase lag for a pure rotary current are related by:

$$\Phi = \text{Cos}^{-1}\left(\frac{B}{A}\right) \qquad (21)$$

Φ = phase lag

B = amplitude of berg velocity vectors

A = amplitude of current vectors

Using the observed value for B/A of .499, a value of 60.1 degrees is obtained for Φ. Thus the observed results are in qualitative agreement with theoretical values. The difference in values is likely caused by the vertical shear in the transitory components of the current field.

TABLE 5

INTERNATIONAL ICE PATROL WIND DRIFT FACTORS
(After Murray, 1969)

WIND VELOCITY	FACTOR
0 - 5 knots	Negligible
6 -14 knots	.025
15 -29 knots	.03
30 + knots	.035

The icebergs studied had a velocity component about 4% of the wind speed and 25° clockwise from the wind vector. The International Ice Patrol (Murray, 1969) uses a factor which varies with wind speed but averages around 3% with the berg drift 30° to the right of the wind (Table 5). These results compare favorably with the values observed in this study.

It was observed that the iceberg velocity vectors correlated best with current and wind vectors 204 min. (3.4 hrs) and 214 min. (3.6 hrs) earlier. These values likely represent typical times for the observed icebergs to respond fully to changes of current and wind. They are within the range predicted by Smith (1974).

7.4 Conclusion

The behaviour of the icebergs identified by cross-correlation analysis is consistent with the theories and experience of other investigators. Therefore, in spite of the limitations of the data, it is likely that the parameters developed by the model for individual icebergs are valid.

8. CONCLUSION

Vector cross-correlations between iceberg velocity vectors and wind and current velocity vectors at a fixed station can be used to model iceberg drift. An average error of less than 20% can be expected, if the iceberg velocities are correlated with past wind and current data.

The best choice of time lag varies considerably but averages around 3.5 hours. This suggests that correlation with past wind and current data is a feasible method for forecasting of iceberg drift.

The study has shown that the detailed behaviour of an iceberg is highly individual but, that in general, the icebergs studied:

1. moved 2.5 times faster, but in the same direction as, the mean current experienced by the iceberg at a depth of 13 meters.
2. had a transitory velocity component which equalled 0.5 of the transitory current experienced by the iceberg at a depth of 13 m and lagged by 73°.
3. had a wind-induced velocity component equal to 4% of, and 25° degrees to the right of, the wind velocity.

REFERENCES

1. Ainslie, A., and J., Duval, 1974. "Icebergs and drilling operations", in Canada's Continental Margins and Offshore Petroleum Exploration, eds. C.J. Yorath, E.R. Parker and D.J. Glass, Can. Soc. Petrol. Geol., Memoir 4.

2. Allen, J.H., et al, 1972. "Iceberg Study, Saglek Labrador" including "Cruise Report C.S.S. Dawson August 7 to August 26, 1972", Faculty of Engineering Report, Memorial University of Newfoundland.

3. Bedford Institute of Oceanography, 1972, Log Book of C.S.S. Dawson August 7 to August 26, 1972, Unpublished.

4. Bruneau, A.A., 1973. "Icebergs over the Canadian continental shelf" proc. CSEG National Convention.

5. Bruneau, A.A., and Dempster, R.T., 1972. "Engineering and economic implications of icebergs in the North Atlantic" Oceanology International 1972.

6. Dempster, R.T., 1974. "The measurement and modelling of iceberg drift", presented at Ocean '74, Halifax, N.S., August, 1974.

7. Dempster, R.T., and A.A. Bruneau, 1973. "Dangers presented by icebergs and protection against them", Arctic Oil and Gas: Problems and Possibilities Conference, Le Havre, France, May 2 - 5, 1973.

8. Durdle, N., 1969. Digital Filtering of Dynamic Physiological Images, M. Eng. thesis, Nova Scotia Technical College, Halifax, Nova Scotia.

9. Haltiner, G.J., and F.L. Martin, 1957. Dynamical and Physical Meteorology, McGraw-Hill.

10. Holden, B., 1974. Some Observations on the Labrador Current at Saglek, Labrador, Master of Engineering project report, Memorial University of Newfoundland, St. John's, NFLD.

11. Murray, J.E., 1969. "The Drift, deterioration and distribution of icebergs in the North Atlantic Ocean" Ice Seminar, CIMM Special Vol. No. 10.

12. Neumann, G. and Pierson, W.J., 1966. Principles of Physical Oceanography, Prentice-Hall, Inc.

13. Smillie, K.W., 1966. An Introduction to Regression and Correlation, Ryerson Press, Toronto.

References (Cont'd)

14. Smith, E.H., 1931. The Marion Expedition to Davis Strait and Baffin Bay, Bulletin no. 19, U.S. Treasury Dept., Coast Guard, U.S. Govt. Printing Office, Washington.

15. Smith, S.D., and E.G., Banke, 1974, "Wind drift and water drag of icebergs", Atlantic Oceanographic Laboratory Contribution XXX, Atlantic Oceanographic Laboratory, Bedford Institute, Dartmouth, N.S.

16. Soulis, E.D., 1974, "Modelling of drift of nearby icebergs using wind and current measurements at a fixed station"; in Canada's Continental Margins and Offshore Petroleum Exploration, eds. C.J. Yorath, E.R. Parker and D.J. Glass; Can. Soc. Petrol. Geol., Memoir 4.

APPENDIX A

RESPONSE OF AN ICEBERG TO A PURE ROTARY CURRENT

With reference of Figure A-1, consider an iceberg moving only under the influence of a uniform pure rotary current represented by:

$$\underline{c} = A \sin wt\,\hat{i} + A \cos wt\,\hat{j} \qquad \text{(A1)}$$

$\underline{c}$ = current velocity

A = current velocity amplitude

t = time

w = period of rotation

The equation of motion for the iceberg is:

$$\dot{\underline{v}} = k|\underline{c} - \underline{v}|(\underline{c} - \underline{v}) \qquad \text{(A2)}$$

$\underline{v}$ = iceberg velocity

$\dot{\underline{v}} = d\underline{v}/dt$

k = a coefficient of drag

The steady state solution for the iceberg's velocity, $\underline{v}$, will occur when the iceberg is experiencing no radial acceleration, that is:

$$\dot{\underline{v}} \cdot \underline{v} = 0 \qquad \text{(A3)}$$

Therefore $\underline{c} - \underline{v}$ is perpendicular to $\underline{v}$ and triangle $P_1 P_2 P_3$ in Figure A-1 is right-angled. If:

$$\underline{v} = B \sin w(t+\tau)\,\hat{i} + B \cos w(t+\tau)\,\hat{j} \qquad \text{(A4)}$$

τ = iceberg velocity time lag

B = iceberg velocity amplitude

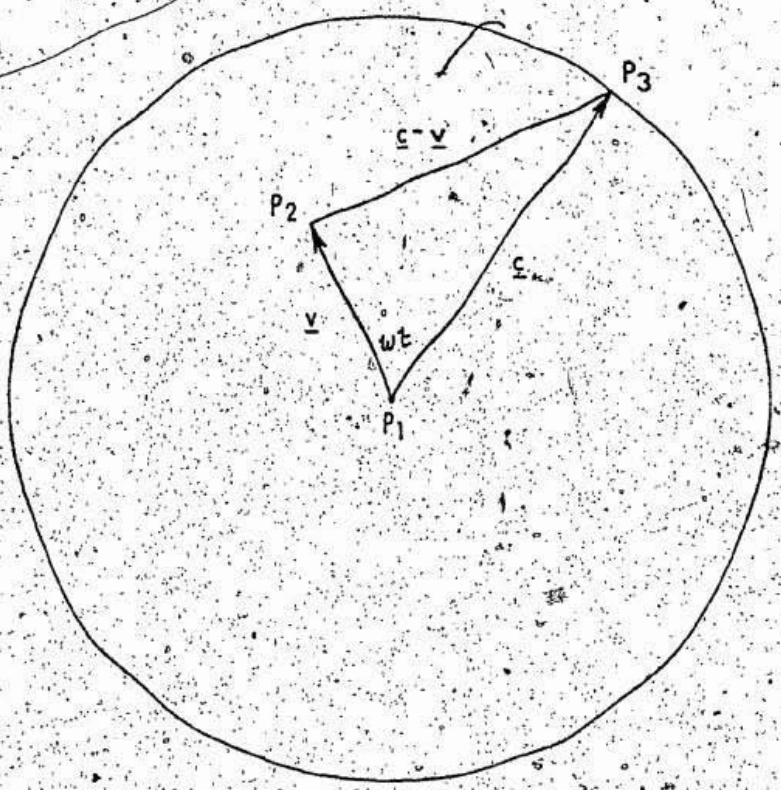

VELOCITY VECTORS FOR CIRCULAR MOTION

Figure A-1

then:

$$\cos w\tau = B/A \tag{A5}$$

Similarly

$$|\underline{c} - \underline{v}|^2 = A^2 - B^2 \tag{A6}$$

From equation (A2)

$$\dot{\underline{v}} \cdot \dot{\underline{v}} = k^2 |\underline{c} - \underline{v}|^4 \tag{A7}$$

From equation (A4)

$$\dot{\underline{v}} = wB \cos w(t+\tau) - wB \sin w(t+\tau) \tag{A8}$$

Therefore:

$$\dot{\underline{v}} \cdot \dot{\underline{v}} = w^2 B^2 \tag{A9}$$

Combining equations (A7), (A8), and (A9) gives:

$$w^2 B^2 = k^2 (A^2 - B^2)^2 \tag{A10}$$

which may be rearranged to give:

$$k_g = wB/(A^2-B^2) \qquad \text{(A11)}$$

To solve equation (A10) for B:

$$kB^2 + wB - kA^2 = 0$$

$$B^2 + \frac{w}{k}B - A^2 = 0$$

$$B = \frac{w}{2k} \pm \left(\frac{w^2}{4k^2} + 1\right)^{1/2}$$

Since B must be greater than zero:

$$B = -\frac{w}{2k} + \left(\frac{w^2}{4k^2} + 1\right)^{1/2} \qquad \text{(A12)}$$